# Long Distance, Unconditional Teleportation of Atomic States via Complete Bell State Measurements

S. Lloyd, M. S. Shahriar, and J. H. Shapiro
*Research Laboratory of Electronics, Massachusetts Institute of Technology, Cambridge, Massachusetts 02139*

P. R. Hemmer
*Air Force Research Laboratory, Sensors Directorate, Hanscom Air Force Base, Massachusetts 01731*
(Received 6 October 2000; revised manuscript received 23 May 2001; published 27 September 2001)

We propose a scheme for creating and storing quantum entanglement over long distances. Optical cavities that store this long-distance entanglement in atoms could then function as nodes of a quantum network, in which quantum information is teleported from cavity to cavity. The teleportation is conducted unconditionally via measurements of all four Bell states, using a novel method of sequential elimination.

DOI: 10.1103/PhysRevLett.87.167903 PACS numbers: 03.67.Hk, 03.67.Lx, 32.80.Qk

This paper proposes a robust scheme for constructing a quantum network [1]. A method is developed for creating entanglement between two distant atoms using entangled photons. These atoms can exchange quantum information by the process of teleportation [2]. Quantum information processing needs only to be performed locally. The scheme should allow reliable transmission of quantum information between quantum microcomputers separated by distances of tens of kilometers, without using entanglement purification or quantum error correction [3,4].

In general, it is difficult to create a quantum wire [5]. Direct quantum communication is fragile; existing methods for coping with noisy quantum channels are complicated and time consuming [6]. The solution is to create a quantum network that does not require reliable quantum wires [7]. Cavity quantum electrodynamics provides mechanisms for communicating between cavities [1,7]. The key technology proposed here is a method for transmitting entanglement over long distances, capturing it in optical cavities, and storing it in atoms.

We describe the method in general terms and provide details later. We use parametric downconversion to create pairs of momentum- and polarization-entangled photons, sending one to cavity 1 and the other to cavity 2, which are equidistant from the source. Each cavity contains an atom, trapped in an optical potential. Because of momentum entanglement, each of the entangled pair of photons arrives at its respective cavity at the same time. Although many of the photon pairs will fail to arrive at and enter their respective cavities, on occasion a photon will enter cavity 1 and its entangled pair photon will enter cavity 2 at the same time. Once in the cavity, the photon can drive a transition between the $A$ and the (degenerate) $B$ levels of the atom [Fig. 1(a)]. This effectively transfers the photon entanglement to the degenerate $B$ levels of the atoms in cavities 1 and 2.

This entanglement can be detected and stored as follows: Concentrate first on a single cavity. To protect the quantum information when the atom has absorbed the photon, drive a transition from $B$ to the long-lived $D$ levels [Fig. 1(a)]. Now detect if the atom has absorbed a photon by driving a cycling transition from $A$ to $C$. If no fluorescence is seen, then the atom successfully absorbed the photon, and the resulting entanglement in $D$ will be stored for subsequent manipulations. Otherwise, the atom was still in $A$, which means it failed to absorb the photon. In this case the atom will return to $A$, ready to absorb the next photon entering the cavity. When the keeper of cavity 1 has captured a photon, she calls the keeper of cavity 2 to see whether he has captured a photon at the same time. If not, she returns her atom to $A$ and tries again. If both cavities have captured a photon at the same time, however, they now possess two entangled distant atoms.

Let us now look at how such a scheme might be carried out using rubidium atoms [Fig. 1(b)]. A UV laser will be used to excite a nonlinear crystal. This crystal will produce pairs of entangled photons, via type-II parametric downconversion, each at 795 nm. An ultrabright, narrow-band parametric amplifier version of this source is described in Ref. [8]. We consider the polarization entanglement to be of the form $(|\sigma_+\rangle_1|\sigma_-\rangle_2 + \exp(i\kappa)|\sigma_-\rangle_1|\sigma_+\rangle_2)/\sqrt{2}$,

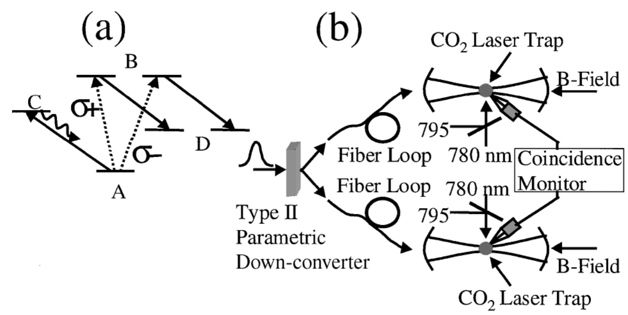


FIG. 1. Schematic illustration of the proposed experiment for creating potentially long distance entanglement between a pair of trapped rubidium atoms (see text).

  

where $\sigma_+$ ($\sigma_-$) indicates right (left) circular polarization. The protocol will work for any known value of $\kappa$. Each beam is coupled into a fiber, and transported to an optical cavity with slow decay and a strong vacuum Rabi frequency (20 MHz) [9].

Each cavity holds a rubidium atom, confined by a focused $CO_2$ laser. The mean number of atoms caught is controlled via the parameters involved in the process, and can be reduced to one in a controlled fashion. It has been demonstrated recently [10] that, at a pressure of $10^{-11}$ Torr, atoms survive for more than 2 min in a $CO_2$ trap. The trap lifetime may be increased up to 1 h by housing the trap chamber in a liquid helium cryostat. In practice, other processes such as fluctuations in the residual magnetic field will limit the decoherence time to a few minutes.

Figure 2 illustrates the transition to be employed in each cavity. Initially, the atom(s) is prepared in the $F = 1$, $m_F = 0$ ground state ("$A$" level). The photon excites the dashed transitions to the $F = 1$, $m_F = \pm 1$ excited level ("$B$" levels) [Fig. 2(a)]. A $\pi$ polarized beam completes the Raman excitation, producing a superposition of the $F = 2$, $m_F = \pm 1$ states ("$D$" levels). To determine if the photon has been absorbed by the atom, the $F = 1$ state is detected by exciting the cycling transition ("$A$ to $C$") shown in Fig. 2(b).

The dual-OPA (optical parametric amplifier) source of Ref. [8] is capable of producing $\sim 10^6$ entangled pairs/sec at 795 nm in $\sim$30 MHz bandwidth. For long distance transmission, one can generate $\sim 10^6$ pairs/sec in the 1550 nm low-loss fiber transmission window. After fiber propagation we can shift the entanglement to the 795 nm via quantum-state frequency translation, previously demonstrated by Huang and Kumar [11].

Quantum communication may be carried out via the following clocked protocol. Time slots of signal and idler (say, 400 ns long) are transmitted down optical fibers to the quantum memories. These slots are gated into the memory cavities, with their respective atoms either physically displaced or optically detuned so that no $A$-to-$B$ absorptions occur. After a short loading interval (a few cold-cavity lifetimes, say, 400 ns), each atom is moved (or tuned) into the absorbing position and $B$-to-$D$ pumping is initiated. After about 100 ns, coherent pumping ceases and the $A$-to-$C$ transition is repeatedly driven (say, 30 times, taking nearly 1 $\mu$s). By monitoring a cavity for the fluorescence from this cycling transition, we can reliably detect whether or not a 795 nm photon has been absorbed by the atom in that cavity. If neither atom or if only one atom has absorbed such a photon, then we cycle both atoms back to their $A$ states and start anew. If no cycling-transition fluorescence is detected in either cavity, then, because we have employed enough cycles to ensure very high probability of detecting that the atom is in its $A$ state, it must be that both atoms have absorbed 795 nm photons and stored the respective qubit information in their $D$ levels.

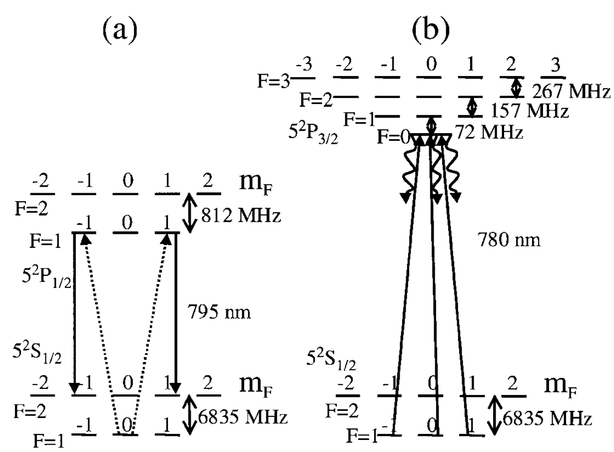


FIG. 2. Schematic illustration of the steps to be used in storing quantum coherence in a rubidium atom, and detecting it nondestructively (see text).

We expect that this loading protocol can be run at rates as high as $R = 500$ kHz, i.e., we can get an independent try at loading an entangled photon pair into the two memory elements of Fig. 1 every 2 $\mu$s. With a high probability, $P_{es}$, any particular memory-loading trial will result in an erasure, i.e., propagation loss and other inefficiencies combine to preclude both atoms from absorbing photons in the same time epoch. With a small probability, $P_s$, the two atoms will absorb the photons from a single polarization-entangled pair. With a much smaller probability, $P_{er}$, both atoms will have absorbed photons but these photons will not have come from a single polarization-entangled pair; this is the error event. In terms of $\{R, P_{es}, P_s, P_{er}\}$ it is easy to identify the key figures of merit. Propagation losses and other inefficiencies merely increase $P_{es}$, and hence reduce the throughput, i.e., the number of successful entanglement loadings per second, $N_s = RP_s$, that could be achieved if the quantum memories each contained a lattice of trapped atoms for sequential loading of many pairs. It is the loading errors, which occur with probability $P_{er}$, that provide the ultimate limit on the entanglement fidelity. This loss-limited fidelity is given by $F_{\max} = I - P_{er}/2(P_s + P_{er})$, where we have assumed that the error event loads independent, randomly polarized photons into each memory.

To quantify the loss-limited throughput and entanglement fidelity of this protocol, one must examine the behavior of the dual-OPA source, along with the excess losses in the OPA cavities and the propagation loss in the fiber. The details of this analysis are presented in Ref. [12]. Here, we summarize the important results. First, it is shown that this source does indeed produce the singlet state, corresponding to $\kappa = \pi$, which has the requisite form of entanglement. Specifically, with no pump depletion and no excess noise, the photons in modes 1 and 2 are found to be in the entangled Bose-Einstein state. When the average photon number per mode ($N$) is much less than unity, this state reduces to

$$|\Psi\rangle_{1,2} \approx (N+1)^{-1}|0\rangle_{1+}|0\rangle_{2-}|0\rangle_{1-}|0\rangle_{2+} + [N(N+1)^{-3}]^{1/2}(|1\rangle_{1+}|1\rangle_{2-}|0\rangle_{1-}|0\rangle_{2+} - |0\rangle_{1+}|0\rangle_{2-}|1\rangle_{1-}|1\rangle_{2+}),$$

i.e., it is predominantly vacuum, augmented by a small amount of the singlet state. Here, for example, the state $|1\rangle_{2+}$ represents a single photon in mode 2, with polarization $\sigma_+$, and so on. Second, the effects of excess loss within the OPA cavity, propagation loss along the fibers, and the coupling loss into the memory cavities can be analyzed in a straightforward manner. The photons inside the memory cavities are now in a mixed state, described by density operators. The parameters determining the fidelity and the throughput of the protocol can be expressed in terms of these density operators as follows:

$$P_{es} = ({}_{1+}\langle 0|\hat{\rho}_{1+}|0\rangle_{1+})({}_{1-}\langle 0|\hat{\rho}_{1-}|0\rangle_{1-}) + ({}_{2+}\langle 0|\hat{\rho}_{2+}|0\rangle_{2+})({}_{2-}\langle 0|\hat{\rho}_{2-}|0\rangle_{2-}) - ({}_{1+}\langle 0|{}_{2-}\langle 0|\hat{\rho}_{1+2-}|0\rangle_{2-}|0\rangle_{1+})({}_{1-}\langle 0|{}_{2+}\langle 0|\hat{\rho}_{1-2+}|0\rangle_{2+}|0\rangle_{1-}),$$

$$P_s = ({}_{12}\langle\psi|\hat{\rho}_{12}|\psi\rangle_{12}), \quad \text{with } |\psi\rangle_{12} \equiv (|1\rangle_{1+}|1\rangle_{2-}|0\rangle_{1-}|0\rangle_{2+} - |0\rangle_{1+}|0\rangle_{2-}|1\rangle_{1-}|1\rangle_{2+})/\sqrt{2}$$

and $P_{er} = 1 - P_{es} - P_s$.

We calculated these quantities under the following assumptions: (i) OPA's pumped at 1% of their oscillation threshold, (ii) 0.2 db/km loss in each fiber, (iii) 5 dB excess loss along each path, accounting for all loss mechanisms other than the propagation loss in the fibers, (iv) a ratio of 0.5 between the linewidths of the OPA cavities and the memory cavities, and (v) a cycling rate of 500 kHz. Under these assumptions, we have found that the throughput $N_S$, in units of pairs/sec, is given by $\log_{10}N_S \approx 3.3 - 0.02d$, where $d$ is the distance, in km, between Bob and Alice. The fidelity, $F_{\max}$, stays close to 97% for a distance up to $d = 100$ km [12].

The entanglement produced this way can be used for quantum teleportation, quantum cryptography, or remote phase measurement [13], for example. Here, we show an explicit construction for performing the teleportation of a quantum state (Fig. 3). The entangled atoms are atom 2 (with Alice) and atom 3 (with Bob). Alice has a third atom (atom 1), whose quantum state she will teleport. Atom 1 is trapped in another node of the $CO_2$ beam, and shares a second cavity with atom 2 [Fig. 3(a)]. We adopt the abbreviated state designations for the $5^2S_{1/2}$ sublevels: $|a\rangle \equiv |F = 2, m_F = -1\rangle$, $|b\rangle \equiv |F = 2, m_F = +1\rangle$, $|c\rangle \equiv |F = 1, m_F = -1\rangle$, and $|d\rangle \equiv |F = 1, m_F = +1\rangle$.

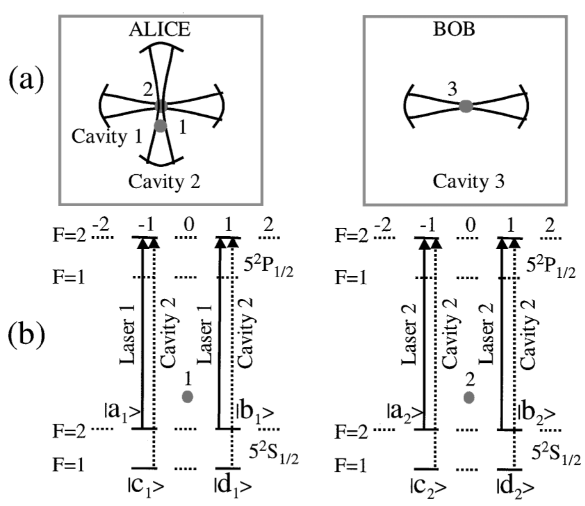


FIG. 3. Teleportation using trapped Rb atoms: (a) Atom 2 (with Alice) and atom 3 (with Bob) are entangled via storage of the entangled photon pairs, as described above. Atom 1 (also with Alice) is held by a second $CO_2$ laser node, and shares a common cavity that is orthogonal to the one used for capturing the entangled photons. (b) Basic model for Alice to transfer the coherence from atom 1 to atom 2, in preparation for teleportation.

Without loss of generality, we choose to write the state of atoms 2 and 3 as $|\psi_{23}\rangle = \{|a\rangle_2|b\rangle_3 + |b\rangle_2|a\rangle_3\}/\sqrt{2}$. Alice can put atom 1 into an unknown state $|\varphi_1\rangle = \{\alpha|c\rangle_1 + \beta|a\rangle_1\}$ by using an optically off resonant (OOR) Raman pulse of unmeasured duration that couples $|c\rangle_1$ to $|a\rangle_1$. Explicitly, $\alpha(t) = \alpha_0$ and $\beta(t) = \beta_0\theta(t)$, where $\theta(t) = \exp[-i(\omega_M t + \xi)]$, the frequency $\omega_M$ and phase $\xi$ being determined by those of the oscillator used to generate the second Raman frequency from the first. Using the scheme of Pellizzari *et al.* [14], which can be realized by using the transitions shown in Fig. 3(b), Alice transfers the state of atom 1 into atom 2, leaving atom 1 in a pure state $|c\rangle_1$, and atoms 2 and 3 in the state $|\phi_{23}\rangle = \{|A_+\rangle(\alpha_0|b_3\rangle + \beta_0|a_3\rangle) + |A\rangle(\alpha_0|b_3\rangle - \beta_0|a_3\rangle) + |B_+\rangle\times(\beta_0|b_3\rangle + \alpha_0|a_3\rangle) + |B\rangle(-\beta_0|b_3\rangle + \alpha_0|a_3\rangle)\}/2$, where the effective Bell basis states are given by $|A_\pm\rangle = \{|c_2\rangle \pm \theta|b_2\rangle\}/\sqrt{2}$ and $|B_\pm\rangle = \{|d_2\rangle \pm \theta|a_2\rangle\}/\sqrt{2}$.

To measure these Bell states, Alice first applies a set of pulses that maps the Bell states to bare atomic states. Consider the states $|A_\pm\rangle$. Alice applies an OOR Raman $\pi/2$ pulse, coupling $|c_2\rangle$ to $|b_2\rangle$, using a $\sigma_+$ polarized light at $\omega_1$ and a $\sigma_-$ polarized light at $\omega_2$, where $\omega_1 - \omega_2 = \omega_M$ [Fig. 4(a)]. The off resonant pulses are tuned near the $F = 1$ excited state to avoid interactions between $|a_2\rangle$ and $|d_2\rangle$. Alice generates $\omega_2$ from $\omega_1$ using an oscillator with a known phase shift of $\xi$. Alice chooses $\xi = -\pi/2$, converting $|A_+\rangle$ to $|c_2\rangle$, and $|A_-\rangle$ to $|b_2\rangle$. Similarly, she applies another OOR Raman $\pi/2$ pulse with different polarizations to convert $|B_+\rangle$ to $|d_2\rangle$, and $|B_-\rangle$ to $|a_2\rangle$.

Alice can now measure the internal states by using a method of *sequential elimination.* First, she applies a Raman pulse to transfer the amplitude of state $|d_2\rangle$ to an auxiliary state in the $5^2S_{1/2}, F = 2$ manifold [Fig. 4(b)].

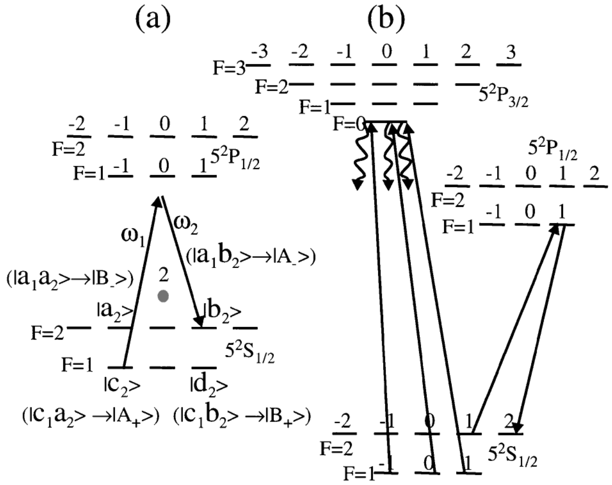


FIG. 4. Bell state measurement: (a) Off resonant Raman transition used to map the amplitudes of the Bell states onto the bare atomic states; (b) Bell state detection is done sequentially using Raman transitions (see text).

A magnetic field can be applied in order to provide the necessary spectral selectivity. Second, she probes the amplitude of state, $|c_2\rangle$, by driving the $5^2S_{1/2}, F = 1$ to $5^2P_{3/2}, F = 0$ cycling transition. If she detects fluorescence, she concludes that the atom is in state $|c_2\rangle$, which in turn means she has measured the Bell state $|A_+\rangle$. If she fails to see fluorescence, she then eliminates this possibility, and now applies a Raman pulse to return the amplitude of the auxiliary state to state $|d_2\rangle$. Alice again drives the cycling transition, and detection of fluorescence implies she has measured the Bell state $|B_+\rangle$. Otherwise, she applies a set of Raman pulses to transfer the amplitude of $|a_2\rangle$ to $|c_2\rangle$ and $|b_2\rangle$ to $|d_2\rangle$. She now repeats the detection scheme for state $|c_2\rangle$. If Alice sees fluorescence, the atom is in $|c_2\rangle$, which implies that she has measured $|A_-\rangle$. If not, she has eliminated three possibilities, which means that the system is in $|B_-\rangle$.

Alice now sends a two-bit classical message to Bob, informing him of which state she has found the world to be in. Bob now has to make some transformations to his atom in order to produce the state $|\phi_1\rangle$ in atom 3. He can accomplish this as follows. If Alice found $|A_+\rangle$, Bob does nothing, and atom 3 is already in state $|\phi_1\rangle$. On the other hand, if Alice found $|A_-\rangle$, then Bob has to flip the phase of $|a_3\rangle$ by $\pi$ with respect to $|b_3\rangle$. This can be achieved by applying an OOR Raman $2\pi$ pulse connecting $|a_3\rangle$ to the auxiliary ground state $|F = 1, m_F = 0\rangle$ via the $|F = 0, m_F = 0\rangle$ state in $5^2P_{3/2}$. Atom 3 is now in state $|\phi_1\rangle$, as desired. If Alice found $|B_+\rangle$, then Bob first applies an OOR Raman $\pi$ pulse coupling $|a_3\rangle$ to $|b_3\rangle$ to swap their amplitudes, again producing the desired state. Finally, if Alice found $|B_-\rangle$, then Bob first applies a $\pi$ pulse as above to swap amplitudes, followed by the $2\pi$ pulse for the $\pi$ phase change, producing the desired state.

This work was supported by AFOSR Grant No. F49620-98-1-0313 and ARO Grants No. DAAG55-98-1-0375 and No. DAAD19-00-1-0177.

[1] J. Cirac *et al.,* Phys. Rev. Lett. **78**, 3221 (1997).
[2] C. Bennett *et al.,* Phys. Rev. Lett. **70**, 1895 (1993).
[3] P. Shor, *Proceedings of the 37th Annual Symposium on the Foundations of Computer Science* (IEEE Computer Society Press, Los Alamitos, CA, 1996), p. 56; D. DiVincenzo and P. Shor, Phys. Rev. Lett. **77**, 3260 (1996).
[4] P. Shor, Phys. Rev. A **52**, R2493 (1995); A. Steane, Phys. Rev. Lett. **77**, 793 (1996); A. Calderbank and P. Shor, Phys. Rev. A **54**, 1098 (1996); R. Laflamme, C. Miquel, J. Paz, and W. Zurek, Phys. Rev. Lett. **77**, 198 (1996); E. Knill and R. Laflamme, Phys. Rev. A **55**, 900 (1997); C. Bennett *et al.,* Phys. Rev. A **54**, 3824 (1996).
[5] S. Lloyd, Science **261**, 1569 (1993).
[6] C. Bennett, D. DiVincenzo, and J. Smolin, Phys. Rev. Lett. **78**, 3217 (1997); B. Schumacher and M. Nielsen, Phys. Rev. A **54**, 2629 (1996); B. Schumacher, Phys. Rev. A **54**, 2614 (1996); S. Lloyd, Phys. Rev. A **55**, 1613 (1997).
[7] S. van Enk, J. Cirac, and P. Zoller, Phys. Rev. Lett. **78**, 4293 (1997).
[8] J. H. Shapiro and N. C. Wong, J. Opt. Soc. Am. B **2**, L1 (2000).
[9] S. Morin, C. Yu, and T. Mossberg, Phys. Rev. Lett. **73**, 1489 (1994).
[10] K. O'Hara *et al.,* Phys. Rev. Lett. **82**, 4204 (1999).
[11] J. M. Huang and P. Kumar, Phys. Rev. Lett. **68**, 2153 (1992).
[12] J. H. Shapiro, in *Proceedings of the Fifth International Conference on Quantum Communication, Measurement, and Computing, Capri 2000,* edited by O. Hirota and P. Tombesi (Plenum, New York, 2001), and references therein.
[13] M. S. Shahriar, quant-ph/001007.
[14] T. Pellizzari *et al.,* Phys. Rev. Lett. **75**, 3788 (1995).